

I give permission for public access to my thesis and for copying to be done at the discretion of the archives' librarian and/or the College library.

Signature

Date

**Regulatory targeting of *Matrix Metalloproteinase 2* by *βtz-f1* in
Drosophila melanogaster fat body remodeling**

by

Alina Vulpe

A Paper Presented to the

Faculty of Mount Holyoke College in

Partial Fulfillment of the Requirements for

the Degree of Bachelors of Arts with

Honor

Department of Biological Sciences

South Hadley, MA 01075

May 2016

This paper was prepared
under the direction of
Professor Craig Woodard
for eight credits

DEDICATION

I wish to dedicate this work to the friends I have made during my time at Mount Holyoke, who have stuck with me for four years and who offered words of comfort when times were hard. I also want to dedicate this thesis to my sister who paved the road into STEM for me.

ACKNOWLEDGEMENTS

I would like to thank the Mount Holyoke College Biological Sciences department for their support, resources and making this project a possibility. I would also like to thank the Mount Holyoke College Lynk program for the financial support over the summer, allowing me to do research without worry.

I want to offer my sincerest gratitude to Professor Craig Woodard, who has been my academic advisor and has offered me valuable insight during my time in college. As well, I want to thank him for allowing me to work in the Woodard Lab, which has served as great scientific experience.

Thank you as well to the other members of my thesis committee, Jason Andras and Darren Hamilton. Thank you for the time and effort you have put into my education. Thank you to Professor Guang Xu from UMass Genomics Lab for the assistance with qPCR reactions.

Thank you to the other Woodard Lab members who were there dissecting fly larvae with me at the oddest of times, who stuck around to help cook fly food, and who have been a valuable source of information and assistance.

Lastly, thank you to Eli and Matilda for hanging out on the couch with me as I type this thesis, offering me unconditional love and support, and a sympathetic ear to my complaining.

TABLE OF CONTENTS

List of Figures.....	viii
List of Tables.....	ix
Abstract.....	x
Introduction.....	1
- <i>Drosophila melanogaster</i> life cycle.....	3
- <i>Drosophila melanogaster</i> larval fat body and metamorphosis.....	5
- Ecdysone (20-hydroxyecdysone).....	7
- β FTZ-F1.....	9
- Regulation of <i>βftz-f1</i> by dBlimp-1.....	12
- MMPs.....	13
- MMPs of <i>Drosophila melanogaster</i>	15
- Hypothesis.....	16
Materials and Methods.....	18
- Experimental design.....	18
- <i>Drosophila</i> genotypes.....	19
- UAS/GAL4 system.....	19
- <i>Drosophila</i> husbandry.....	20
- Virgin collection and experimental crosses.....	21
- Dissection of prepupae.....	21
- RNA isolation.....	22
- Removal of contaminating DNA with DNase treatment.....	23
- First strand cDNA synthesis with Oligo(dT).....	24
- Primer design.....	26
- Reverse Transcriptase PCR (RT-PCR).....	26
- Gel electrophoresis.....	28
- Quantitative Real Time PCR (qPCR).....	29
- Primer optimization.....	30
- Standard curves and efficiencies for qPCR.....	30
- Set up of qPCR plate.....	31
- qPCR data analysis.....	33
Results.....	34
- Observations during dissections.....	34
- Visualization of PCR products via gel electrophoresis.....	35
- Quantitative Real-Time PCR standard curves and primer efficiencies.....	38
- Expression ratios of qPCR results.....	39

Discussion.....	42
- Dissection observations.....	42
- Reverse Transcriptase PCR and gel electrophoresis.....	43
- Quantitative Real-Time PCR results.....	43
- Delayed expression of <i>βftz-fl</i> disrupts normal development.....	46
- Relationship between human health and larval fat body remodeling.....	47
- Matrix Metalloproteinases and human health.....	47
- Conclusion.....	49
- Future directions.....	49
Appendix.....	51
- qPCR plate setup	
- Table of numbered samples corresponding to the genotype and hour of collection.....	52
Literature cited.....	53

LIST OF FIGURES

Figure 1. <i>Drosophila melanogaster</i> life cycle	4
Figure 2. Larval fat body remodeling	5
Figure 3. Diagram of ecdysone pulses during metamorphosis	9
Figure 4. Expression of <i>βftz-f1</i> during metamorphosis	10
Figure 5. qPCR data showing ratio of <i>βftz-f1</i> expression in larval fat body	13
Figure 6. Protein domains of MMPs	14
Figure 7. The <i>UAS/GAL4</i> system	20
Figure 8. Gel	36
Figure 9. Gel	36
Figure 10. Gel	37
Figure 11. Gel	37
Figure 12. Standard curve for <i>Actin5c</i>	38
Figure 13. Standard curve for <i>Mmp2</i>	39
Figure 14. Expression ratios of <i>Mmp2</i> from qPCR experiments	41
Figure 15. Proposed expression levels of MMP2	45

LIST OF TABLES

Table 1. Master mix 1 of cDNA synthesis	24
Table 2. Master mix 2 of cDNA synthesis	25
Table 3. Primer sequences of <i>Actin5c</i> and <i>Mmp2</i>	26
Table 4. RT-PCR reaction mix	27
Table 5. Thermocycler profile for <i>Actin5c</i> and <i>Mmp2</i> RT-PCR amplification	28
Table 6. Optimal primer concentrations (Paplexi, 2013)	30
Table 7. Mix of <i>Actin5c</i> reaction for qPCR	32
Table 8. Mix of <i>Mmp2</i> reaction for qPCR	32
Table 9. qPCR thermocycler profile	33

ABSTRACT

Tissue remodeling is involved in multiple functions in the animal body, as the process through which cells dissociate and detach from each other. Tissue remodeling is the driving force behind wound healing and cancer metastasis, and is carried out partially by Matrix Metalloproteinases (MMPs). MMPs are proteases that degrade the extracellular matrix (ECM) between cells, which then allows them to move freely from one another. The expression of *Mmps* is highly regulated. To study *Mmp* regulation and tissue remodeling, *Drosophila melanogaster* makes for a highly useful model organism due to a process called larval fat body remodeling.

Larval fat body remodeling occurs when *Drosophila* go from larva to adult fly, a highly regulated process thought to involve Matrix Metalloproteinase 2 (MMP2). MMP2 is believed to be the mechanism of ECM fat cell cleaving, which allows for cells to detach from each other and move around freely during larval fat body remodeling. Research suggests that the expression of *Mmp2* in *Drosophila* is 20-hydroxyecdysone (ecdysone) hormonal cascade regulated, mediated by β FTZ-F1 (Bond et al., 2011). Bond et al. (2011) showed that both *β ftz-f1* and *Mmp2* are necessary and sufficient for larval fat body remodeling in *Drosophila*. The hypothesis of this study is that *Mmp2* is a downstream target of β FTZ-F1 in the ecdysone hormonal cascade, more specifically that *Mmp2* expression is induced by β FTZ-F1.

Levels of *Mmp2* expression were relatively quantified compared to a control gene, in wild type *Drosophila* and transgenic *Drosophila* in which expression of *β ftz-f1* was reduced in the larval fat body. To fully sustain my hypothesis, I expect to see reduced expression of *Mmp2* in *β ftz-f1* reduced larval fat body compared to wild type larval fat body. This is because if expression of *Mmp2* is induced by *β ftz-f1* expression, by reducing *β ftz-f1* it comes that there will be a reduction of *Mmp2* expression as well. The findings of this study show a reduction of *Mmp2* at 10 hours after puparium formation (APF) in *β ftz-f1* reduced larval fat body, which is consistent with the hypothesis. At 8 and 12 hours APF, the study found increased expression of *Mmp2*, which does not support the hypothesis, however it might be explained by individual variances in biological samples, as well as a quickly shifting level of *Mmp2* expression at these time points. Future studies using the Western blot technique might serve as a tool to more precisely study expression levels at these time points.

INTRODUCTION

Tissue remodeling is an important mechanism for growth and development in animals. The process is characterized by the cleaving of the connective membrane (extracellular matrix, ECM) between cells by an enzyme, which allows individual cells freedom of motion (Woessner, 1991). Humans also undergo tissue remodeling, as a mechanism for wound healing and in cancer metastasis. In the case of cancer metastasis, diseased cells migrate from the tumor, and can relocate to other parts of the body through blood vessels (Malemud, 2006; Hyun and Parks, 2007). For wound healing, tissue remodeling comes into play in order to break down the ECM around damaged cells around the wound so that they can be transported away from the wound site, as well as breaking down the ECM of healthy cells in the area to allow for better integration of new tissue (Stevens and Page-McCaw, 2012). Enzymes called Matrix Metalloproteinases (MMPs) degrade the ECM during tissue remodeling. MMPs are important subjects of study in attempting to provide a method of inhibition to cancer metastasis, by inhibiting their activity (Hyun and Parks, 2007).

Drosophila are amazing model organisms due to their short generation time, their availability and ease of culture, as well as the fact that we share some homologous genes with them. According to Reiter et al. (2001), homologs of 77% of human disease genes had homologs in *Drosophila*. It is for these reasons that *Drosophila* are so widely used for research impacting humans. When *Drosophila*

undergoes metamorphosis, most of its larval organs undergo programmed cell death in order for new adult ones to form. An organ called the larval fat body goes through tissue remodeling during metamorphosis, and is spared from programmed cell death (Bond et al., 2011). The fat body is a collection of polygonal shaped cells connected in sheets, but during remodeling the individual cells detach and take on a spherical shape (Bond et al., 2011). The larval fat body is kept by the organism as an energy source for the larva/pupa during metamorphosis, as it is the storage unit for all the nutrients gathered during the feeding stages (Aguila et al., 2007). After the larva matures into an adult, the remaining fat body cells are replaced by adult fat body sheets, which are not as readily accessible by the fly (Aguila et al., 2007).

Previous research has shown that metamorphosis is driven by ecdysone, a steroid hormone, and its active metabolite, 20-hydroxyecdysone, and for ease of reading, they will be referred to as ecdysone (Agawa et al., 2007). The events of the first 12 hours of metamorphosis are directed by two pulses of ecdysone, the late-larval pulse and the prepupal pulse (Agawa et al., 2007). Both of these ecdysone pulses regulate the transcription of regulatory “early genes”, which in turn induce the transcription of “late genes”, which are located downstream. Fat body remodeling is induced by the prepupal ecdysone pulse (Agawa et al., 2007). There is also a period in between these two pulses, called the “mid-prepupal” period, in which the concentration of ecdysone is low (Woodard et al., 1994). Of the genes expressed at this “mid-prepupal” period, *βftz-fl* is an essential

regulatory gene, and its product plays the role of a competence factor for the “early genes” to respond to the prepupal ecdysone pulse, including the genes active in fat body remodeling (Woodard et al., 1994).

***Drosophila melanogaster* life cycle**

Life for *Drosophila* begins at egg fertilization, with the embryo developing during embryogenesis and hatching into a larva within one day. There are five stages in the life cycle of *Drosophila*: embryonic, larval, prepupal, pupal and adult (Figure 1). During the larval stage, which lasts 4 days, the animal goes through three stages: the first, second and third instar. They are separated by molting or shedding of the exoskeleton in order to continue growing. During the larval stage, the larva will eat enough food in order to increase its body mass 200 times (Aguila et al., 2007). The nutrients it gathers are then stored in the larval fat body in order to provide the animal with the necessary energy for undergoing metamorphosis, when it cannot eat (Aguila et al., 2007).

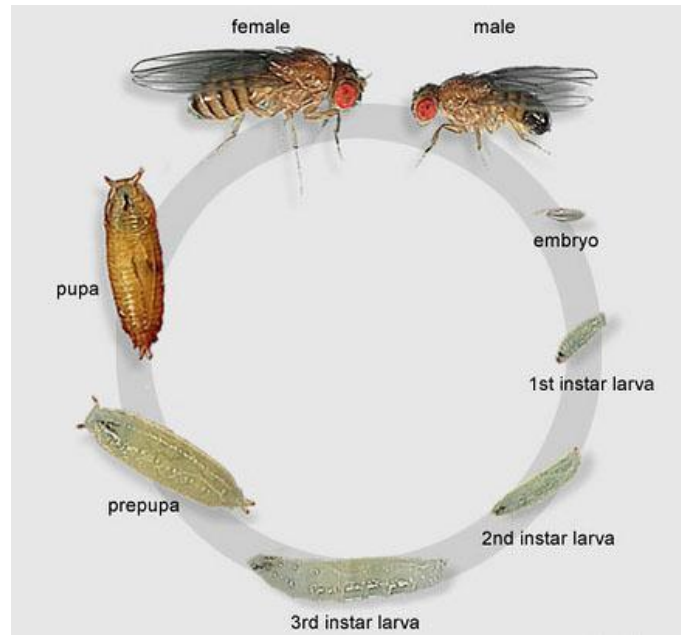


Figure 1: *Drosophila melanogaster* life cycle. The five life stages of *Drosophila melanogaster*: embryonic, larval (divided into first, second and third instar), prepupal, pupal and adult fly (Weigmann et al., 2003).

When the larva reaches optimal body mass, it leaves the food surface for 12-24 hours to find a smooth surface to attach to and undergo puparium formation (Aguila et al., 2007). Once a suitable location is found, movement ceases and puparium formation begins. This is what is called a zero hour prepupa, and it remains so for a very short time, about 15-30 minutes, before puparium formation is complete (Bainbridge and Bownes, 1981). *Drosophila* goes from prepupa to pupa about ten to twelve hours after puparium formation, an event that is marked by the eversion of the head capsule (Bond et al., 2007). It is at this point that the majority of larval structures are destroyed, and the larval fat body undergoes tissue remodeling. The adult fly emerges from the pupal casing 3.5-4.5 days later.

***Drosophila melanogaster* larval fat body and metamorphosis**

The larval fat body is an extremely important structure for *Drosophila*, as it serves the same purpose as liver and fat tissue do in humans: storage of nutrients and metabolizing energy, providing nourishment to the animal as it undergoes metamorphosis (Søndergaard, 1993; Hoshizaki, 2005; Aguila et al., 2007; Liu et al., 2009). It also is involved in the fly's metabolism, with sensors measuring the level of nutrients available and signaling the brain to release insulin-like peptides (Géminard et al., 2009). While most of the larva's organs and tissues are destroyed during metamorphosis by programmed cell death, the larval fat body undergoes remodeling, providing the metamorphosing animal with energy as it transitions and into early adult fly (Aguila et al., 2013). The fat body is a collection of polygonal shaped cells connected in sheets, but during remodeling the individual cells detach and take on a spherical shape (Bond et al., 2011) (Figure 2).

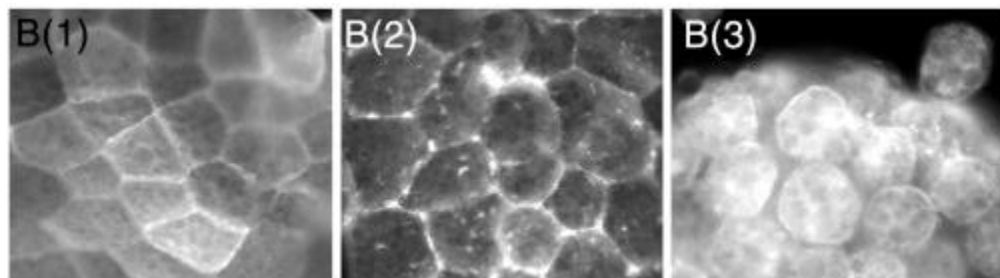


Figure 2. Larval fat body remodeling. B(1) shows the attached sheet of polygonal shaped cell structure of the larval fat body. B(2) shows the fat body at the beginning of remodeling, in which the cells of the fat body are beginning to individualize and take on a more spherical appearance. In B(3) we see the larval fat body dissociating and spherical (Bond et al., 2011).

Fat body remodeling happens in three stages: retraction, disaggregation, and detachment. During retraction, at about 6 hours APF (after puparium formation), the fat body cells are pushed backwards in the animal, towards the abdomen (Hoshizaki, 2005). The disaggregation stage is characterized by the rounding of the cells and slight separation caused by loss of cell-cell adhesion, and detachment occurs at the transition from prepupa to pupa. At the detachment stage we observe slight contractions happening in the larval body, which are followed by the movement of a gas bubble and stronger abdominal contractions, leading to the eversion of the head (Hoshizaki, 2005; Bond et al., 2011). The dissociated fat body cells are now free to move throughout the body cavity, some moving towards the head capsule (Bond et al., 2011). Eventually, the larval fat body cells undergo programmed cell death, but only after the adult has emerged from the pupal casing and has found an alternate source of food (Nelliot et al., 2006). After coming out of the pupal case, it takes a young adult fly roughly 8 hours before its wings extend and it can fly and find an alternate source of nutrients. The fact that the larval fat body is still present in this young adult fly is crucial to its survival until such reliable food source is found (Aguila et al., 2007). After the larval fat body cells are reabsorbed, they get replaced by adult fat body cells, which still store nutrients but which are not as readily available to the fly as those of the larval fat body (Aguila et al., 2007).

Ecdysone (20-hydroxyecdysone)

Research has shown that ecdysone and its active form 20-hydroxyecdysone regulate metamorphosis (Agawa et al., 2007) (ecdysone and its metabolite will be collectively referred to as ecdysone). In order to regulate the expression of genes, ecdysone must first bind to its receptor, which consists of two nuclear receptors: EcR (NR1H1) and USP (Ultraspiracle, NR2B4) (Kozlova and Thummel, 2003; Bond et al., 2011). Damage or loss of these ecdysone receptors or loss of ecdysone is lethal to the animal (Kozlova and Thummel, 2003). Six major pulses of ecdysone govern the control of embryogenesis, molting and metamorphosis in *Drosophila*, as well as three minor pulses that happen before metamorphosis in the third instar larval phase (Ou and King-Jones, 2013). Ecdysone expression targets almost all organs at some point in development, and tissue specificity is required in order to provide the adequate developmental effects at the right time (Spindler et al., 2009). This specificity is provided by the ecdysone signaling cascade (Bond et al., 2011). Ecdysone is necessary in larval fat body remodeling, with the loss of ecdysone signaling causing non-dissociation of the fat cells (Bond et al., 2011). This shows that ecdysone is necessary during the disaggregation and detachment phases (Bond et al. 2011). The increase and decrease of the ecdysone titer conveys temporal specificity to gene expression, which regulates metamorphosis in the *Drosophila* (Woodard et al., 1994). The increase in the ecdysone titer (ecdysone pulse) leads to an increase of hormone to ecdysone receptor binding, which in turn leads to the

transcription of genes that trigger the transcriptional cascade (Bond et al., 2011). Occurring late during the third instar phase, the late-larval ecdysone pulse triggers the formation of the puparium and thus marks the beginning of the prepupal stage, while the prepupal ecdysone pulse happens roughly 10-12 hours APF and triggers the transition to pupa and fat body remodeling (Nelliot et al., 2006) (Figure 3). These ecdysone pulses cause the transcription of regulatory “early genes”, whose proteins then induce the transcription of “late genes” which are located downstream (Agawa et al., 2007). During these two ecdysone pulses, there is a moment of low ecdysone titer, called the “mid-prepupal” period and the genes that are transcribed during this period are called mid-prepupal genes (Woodard et al., 1994; Yamada et al., 2000). Of all the genes transcribed at this time, the one important to this research is *βftz-f1*.

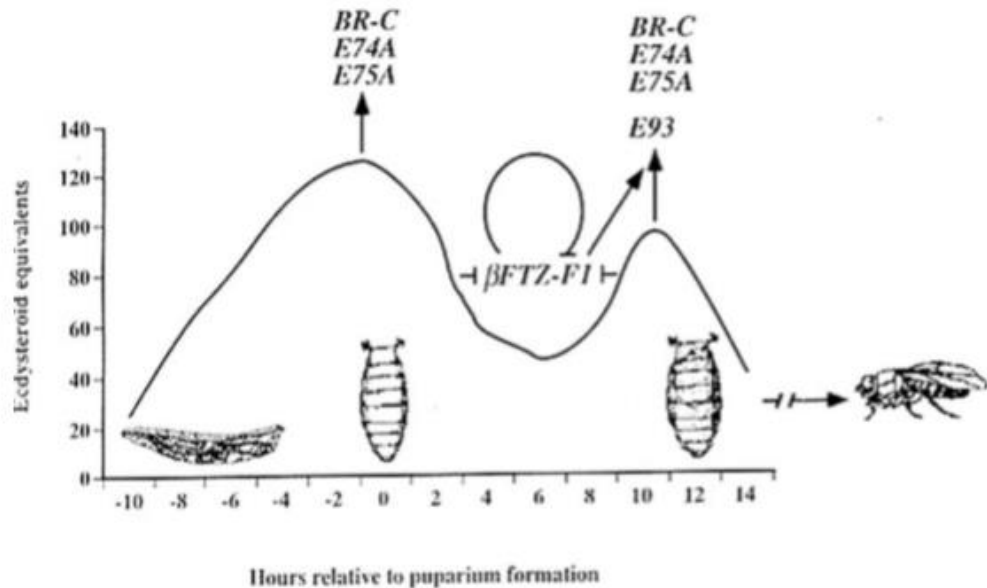


Figure 3. Diagram of ecdysone pulses during metamorphosis. The first peak shows the first, late larval, ecdysone pulse, followed by the mid-prepupal low ecdysone titer stage, and the second, prepupal, ecdysone pulse, signaling fat body remodeling. The diagram also show the early and late genes that are transcribed.

β FTZ-F1

Transcribed during the midprepupal stage, $\beta ftz-f1$ is the subject of this research. $\beta ftz-f1$ encodes one of the isoforms of the Fushi Tarazu Factor-1 (FTZ-F1) protein, while $\alpha ftz-f1$ encoded the other isoform. $\alpha ftz-f1$ is expressed during the embryonic developmental stage (Guichet et al., 1997) and is involved in the development of body segments (Lavorgna et al., 1991). $\beta ftz-f1$ is expressed at the end of embryogenesis, before each larval molt, and also at 6-10 hours APF (Figure 4) (Lavorgna et al., 1991; Woodard et al., 1994).

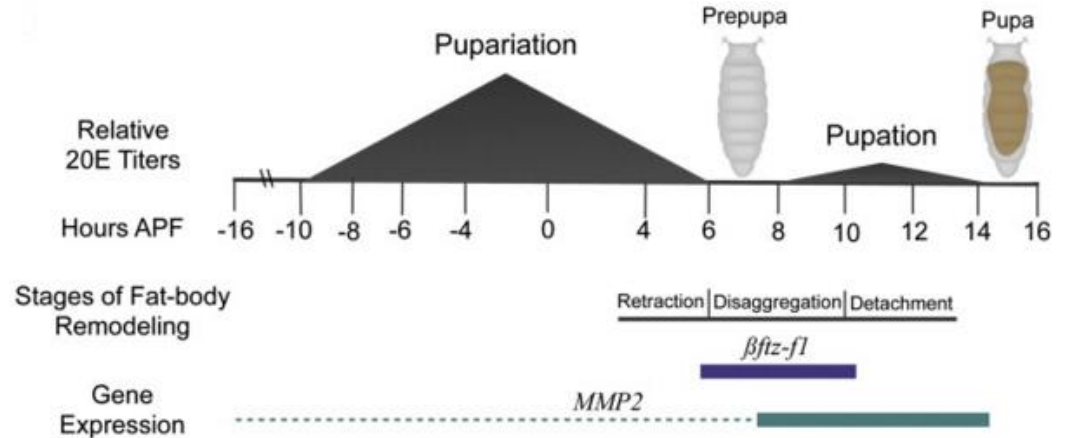


Figure 4. Expression of *betaftz-f1* during metamorphosis. *betaftz-f1* is expressed at 6 and 10 hours APF, when there is a low ecdysone titer. This along with the beginning of increase of ecdysone at pupation, triggers the expression of MMP2. MMP2 is the driver of fat body remodeling, cleaving the ECM holding the fat body cells in sheets and thus allowing the individual cells to move independently.

The β FTZ-F1 protein product is the competence factor that provides certain genes with the ability to respond to the prepupal ecdysone pulse (Woodard et al., 1994.). One such gene that requires β FTZ-F1 is *E93*, which is necessary for programmed cell death (Lee et al. 2002). β FTZ-F1 binds to *E93* at the 3' prime end of its first intron, and in doing so may enable *E93* to respond to the ecdysone pulse (Shresthak, 2005). *betaftz-f1* mutants respond normally to the first ecdysone pulse (late-larval), but show an altered response during the prepupal ecdysone pulse (Broadus et al., 1999). Ectopic expression of *betaftz-f1* before the first ecdysone pulse leads to higher levels of mRNA from genes that we would normally see expressed after the second ecdysone pulse (Woodard et al., 1994). These results are consistent with β FTZ-F1 as a competence factor.

βftz--f1 is also the only known mid-prepupal gene that is necessary for the genetic response to the prepupal ecdysone pulse (Akagi, Ueda, 2011). Larval fat body remodeling happens as a response to the prepupal ecdysone pulse, not the late larval pulse. The genes responsible for larval fat body remodeling may be other mid prepupal genes or early genes getting their competence from βFTZ-F1. We see premature larval fat body remodeling when *βftz-f1* is expressed prematurely, and a lack of larval fat body remodeling when ecdysone signaling is repressed (Bond et al., 2011). This is because it is impossible for the genes involved late in the larval fat body remodeling to respond to the prepupal ecdysone pulse without *βftz-f1* or in fact be transcribed without ecdysone (Bond et al., 2011). Considering that fat body remodeling happens in response to the prepupal ecdysone pulse, *βftz--f1* is necessary and sufficient for fat body remodeling (Pohl, 2014). It is also involved in controlling other metamorphic changes, such as leg and wing extension (Fortier et al., 2003).

Expression of *βftz--f1* is regulated by ecdysone, dBlimp-1, DHR3 and DHR4. dBlimp-1 is a rapidly degrading protein that is induced by ecdysone and represses the expression of *βftz-f1* (Bond et al., 2011). *dBlimp-1* expression occurs due to the late larval ecdysone pulse, and acts as a repressor to *βftz--f1* transcription by binding to the *βftz-f1* promoter (Bond et al., 2011). Evidence of dBlimp-1 as a repressor of *βftz--f1* is seen in flies that overexpress d-Blimp-1 and thus show a delay in *βftz--f1* expression (Agawa et al.2007; Perez, 2014).

Regulation of *βftz-f1* by dBlimp-1

dBlimp-1, or *Drosophila* Blimp-1, is a protein homologous to the mammalian B-lymphocyte maturation protein-1, and is expressed much like the early genes, induced directly by the ecdysone pulses: a reduced level of *dBlimp-1* when there is a low ecdysone titer (Agawa et al., 2007; Akagi and Ueda, 2011). Alternatively, the protein product of *dBlimp-1* is only present in high levels of ecdysone, which is a rapidly degraded transcription repressor, the mechanism through which ecdysone represses expression of *βftz-f1* (Bond et al., 2011). dBlimp-1 blocks transcription of *βftz-f1* by binding to its promoter (Agawa et al., 2007). Previous research has shown that flies that overexpress *dBlimp-1* in the larval fat body show reduced and delayed expression of *βftz-f1* past its relevant point (Figure 5)(Perez, 2014). If we delay the expression of *βftz-f1* past its relevant point of conferring competency to downstream targets, the concentration of *βftz-f1* past this point is irrelevant, as it will be unable to perform its role as a competence factor and its downstream target will not be able to respond to ecdysone changes. These findings serve as basis for the notion of dBlimp-1 acting as a transcriptional repressor of *βftz-f1* (Perez, 2014), and will be used in this research.

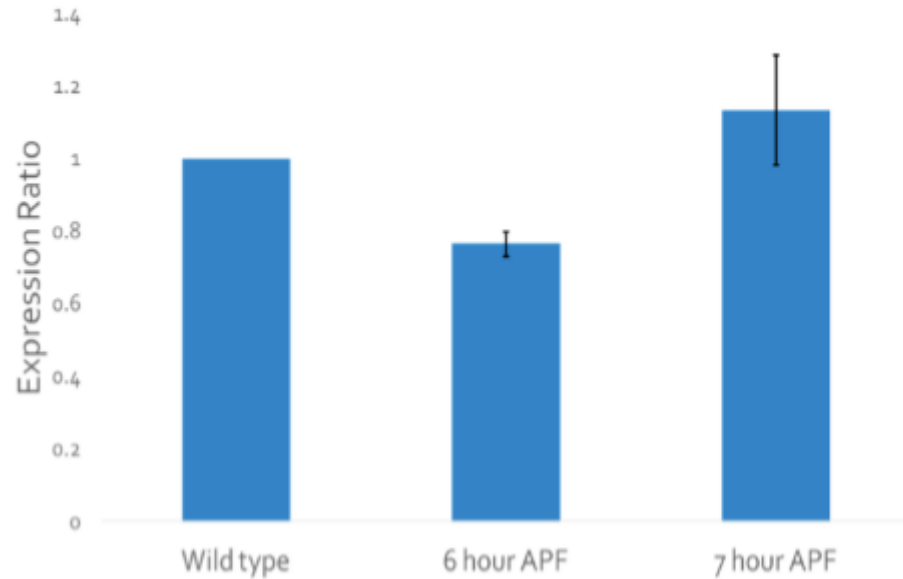


Figure 5. qPCR data showing ratio of $\beta ftz-f1$ expression in larval fat body.

The bar graph shows the ratio of expression of $\beta ftz-f1$ in the larval fat body of *Drosophila* over-expressing *dBlimp-1* at 6 and 7 hours APF in relation to wild-type *Drosophila* (shown here as a value of 1). At 6 hours APF there is underexpression of $\beta ftz-f1$ in flies over-expressing *dBlimp-1*, and we see over-expression of $\beta ftz-f1$ at 7 hours APF. This shows a delay or reduction of expression of $\beta ftz-f1$ in flies over expressing *dBlimp-1* at its point of relevancy, causing $\beta ftz-f1$ to be unable to confer competence to downstream targets (Perez, 2014).

MMPs

MMPs are proteases (zinc-dependent endopeptidases) that break apart the extracellular matrix by cleaving peptide bonds and degrading the collagen fibers (Woessner, 1991; Page-McCaw et al., 2007). They are initially synthesized as inactive pro-enzymes in order to protect against harmful actions of proteases

(Hyun-Jeon and Parks, 2007; Gialeli et al., 2010). It's possible to have this kind of initial inactive synthesis followed by activation thanks to the multi-domain design of the MMP enzyme family (Kessenrock et al., 2010). The three domains of the MMP family are the pro-peptide domain, catalytic domain, and the hemopexin-like domain (Page McCaw et al., 2007; Kessenrock et al., 2010).

The catalytic domain performs the actions of the protein (like ECM protein cleaving) (Page-McCaw et al., 2007), while the pro-peptide domain acts as a self-inhibitor and is what renders the protein inactive after its first translation (Lu et al., 2011). The hemopexin-like domain is involved in interactions with other proteins and is connected to the catalytic domain through a flexible hinge (Figure 6) (Kessenrock et al., 2010' Lu et al., 2011). Initial translation as an inactive enzyme is only one of the regulatory mechanisms of MMPs (Kessenrock et al., 2010).

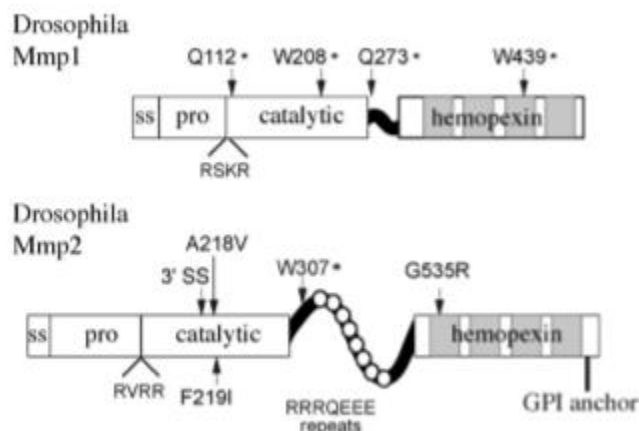


Figure 6. Protein domains of MMPs. The pro-peptide domain is located near the N terminus of the protein and keeps the enzyme in the inactive state upon initial translation. The catalytic domain, located in the center, performs actions of the

protein. The hemopexin-like domain is located at the C terminus of the protein, is connected to the catalytic domain via flexible hinge, and performs protein-protein and protein-cell interactions (Page-McCaw, 2008).

MMPs are involved in developmental processes in the human body, as they are key players in tissue remodeling including organ development and wound healing (Kessenrock et al., 2010). Their study provides vital information for creating treatments for various ailments, including cancer.

MMPs also play a role in the remodeling of *Drosophila* larval fat body. MMP2 acts in the dissociation between individual fat body cells (Qiangpiand et al., 2014). We hypothesize that MMP2 cleaves the ECM proteins which hold the larval fat body cells in sheets, thus allowing them to dissociate and move freely (Bond et al., 2011). In flies mutant for *Mmp2* the fat body does not dissociate, and in the case of early expression, premature fat body remodeling occurs, which is fatal to the animal (Bond et al., 2011).

MMPs of *Drosophila melanogaster*

While there are up to 25 different MMPs in vertebrates (with 24 in mammals), study of their role is challenging (Hyun-Jeong and Parks, 2007). The MMPs in *Drosophila* are not orthologous to vertebrate MMPs, but they do have the same structure and perform similar functions (Bond et al., 2011). While having 25 or 24 MMPs is useful, it proves challenging to study. *Drosophila* have only 2 MMPs, *Mmp1* and *Mmp2* which offers a much simpler and better model for research (Page-McCaw, 2008; Qiangpiang et al., 2014). Previous research did

not find MMP1 involved in larval fat body remodeling, however recently it has been discovered that reduction in expression in either MMP1 or MMP2 can delay dissociation of fat body cells (Jia et al., 2014). MMP2 is the primary MMP involved in fat body remodeling, causing degradation to the extracellular matrix connecting the larval fat body cells.

Hypothesis

Because ecdysone is required for fat body remodeling, blocking ecdysone signaling prevents this process. *Mmp2* expression is induced by the prepupal ecdysone pulse. Premature expression of *Mmp2* results in premature remodeling of the fat body. Blocking ecdysone signaling should reduce *Mmp2* expression in the larval fat body. *βftz-f1* is expressed between the two ecdysone pulses during the mid-prepupal period, and prematurely expressing *βftz-f1* causes an up-regulation of *Mmp2* expression. Both *βftz-f1* and *Mmp2* are necessary and sufficient to induce fat body remodeling. Given this and the fact that early expression of *βftz-f1* causes up-regulation of *Mmp2*, I hypothesize that *βftz-f1* downstream regulates *Mmp2*. I also hypothesize that down-regulating *βftz-f1* in the larval fat body will result in down-regulation of *Mmp2* in the fat body (Bond et al., 2011).

I hypothesize that βFTZ-F1 is a competence factor for *Mmp2* during the mid-prepupal period, making the *Mmp2* gene able to respond to the prepupal ecdysone pulse and be transcribed. *Mmp2* might be a direct downstream target of

βftz-f, as an early gene of the prepupal ecdysone pulse, which gets competence directly from βFTZ-F1 in the mid-prepupal period. It also might be an indirect target, as a late gene of the prepupal ecdysone pulse. As a late gene, it would get competence from an early gene that got transcriptional competence from βFTZ-F1 during the mid-prepupal period.

I expect to see reduced *Mmp2* expression in the larval fat body of *βftz-fl* reduced flies, due to a reduction of βFTZ-F1 not fully giving competence to *Mmp2*. If *Mmp2* is not competent, it will be unable to respond to the prepupal ecdysone pulse (Bond et al., 2011). This in turn would mean MMP2 will not be present in the larval fat body to break down the ECM during the prepupal to pupal transition. A lack of ECM breakdown would result in fat body remodeling being incomplete, missing the disaggregation and detachment stages.

MATERIALS AND METHODS

Experimental design

In order to test the hypothesis, a comparative analysis was done of wild type and transgenic *βftz-fl*-reduced *Drosophila Mmp2* mRNA transcripts expressed in the larval fat body during fat body remodeling. The transgenic flies will show a reduction of *βftz-fl* expression just in the fat body (a full *βftz-fl* mutant would cause the animal not to survive embryogenesis) (Bond et al., 2011). These flies were developed by over expressing *dBlimp-1* in the larval fat body, which has been shown to delay and reduce expression of *βftz-fl* past normal expression time.

Samples of larval fat body were collected from wild-type control and *βftz-fl*-reduced flies at 8, 10, and 12 hours APF and levels of *Mmp2* mRNA transcript were measured. The measurements were done via quantitative real time PCR, which measured initial transcripts present in PCR reactions through relative quantification. Results were computed as a ratio of original *Mmp2* cDNA template to the housekeeping gene *Actin5c* (which is expressed in *Drosophila* in all tissues at high levels) (Pfaffl, 2001). Results are expected to show a reduced level of *Mmp2* mRNA transcript in the transgenic fat body as compared to the control wild type.

***Drosophila* genotypes**

For this study, I used three genotypes: w^{1118} , *cg-Gal4*, and $w; UAS-dBlimp-1(XA)$. w^{1118} flies are white-eyed flies that are otherwise wild type and acted as a control in this study. *Cg-GAL4* and $w;UAS-dBlimp-1(XA)$ *Drosophila* were crossed in order to create the transgenic genotype (*cg-GAL4; w; UAS-dBlimp-1(XA)*). Previous research in the Woodard lab has shown that this specific genotype shows a reduced level of *βftz-fl* expression in the larval fat body (Figure 5) (Perez, 2014). The *UAS/Gal4* system allows for *dBlimp-1* expression in the fat body of *βftz-fl*-reduced flies.

***UAS/GAL4* system**

The system requires a cross between parental flies in which a gene (in this case, *dBlimp-1*) is regulated by the upstream activating sequence (UAS) element of *Saccharomyces cerevisiae*, and parental flies that contain the *GAL4 Saccharomyces cerevisiae* driver under control of tissue specific promoters (in this case, specific to the larval fat body) (Duffy, 2002). In order to transcribe, a gene under control of *UAS* requires a *GAL4* driver (Duffy, 2002). The progeny of these parental flies express the gene that is under *UAS* control (*dBlimp-1*) only in the specific structures of the *GAL4* driver expression pattern (larval fat body) (Figure 7)(Duffy, 2002).

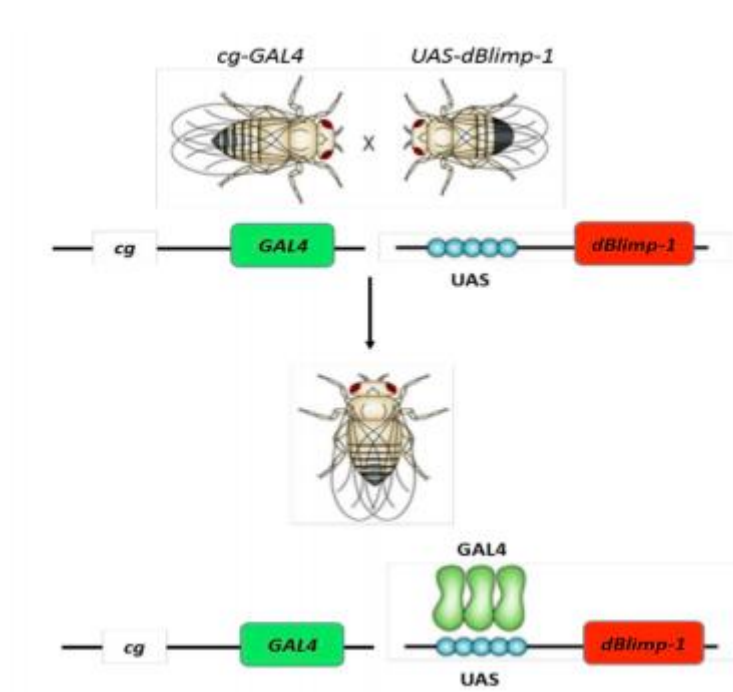


Figure 7. The UAS/GAL4 system. In this study, *dBlimp-1* is the gene under UAS control and requires a *GAL4* driver in order to transcribe correctly, which is provided by the *cg-GAL4* flies. This driver is only present in the larval fat body cells. This means that the progeny of these parental flies will only express *dBlimp-1* in the larval fat body. (St. Johnston, 2002).

***Drosophila* husbandry**

Animals were kept at 25°C with 50% humidity in plastic bottles, with standard *Drosophila* culture medium. This medium is made from water, yeast, agar, malt, corn syrup, and cornmeal. In order to inhibit mold, tegosept and propionic acid are added. Each container was supplemented with a sprinkling of dry yeast before flies were added. In order to keep the stocks healthy and prevent mites, the flies were switched into new bottles every week.

Virgin collection and experimental crosses

Adult flies were removed from bottles that showed a large number of soon to eclose flies and cotton balls were inserted into the bottles, coating the food surface. This provides a clean collection surface. The bottles were incubated at 25°C and virgins were collected after 8 hours. The bottles were also incubated at 18°C and the resulting virgins were available for collection after 18 hours. Collection was done by knocking out flies with CO₂, after which they were sexed and females were kept separate from males in vials.

Crosses were performed as follows: *w; UAS-dBlimp-1(XA)* males to *cg-GAL4* females, and *cg-GAL4* males to *w; UAS-dBlimp-1(XA)* females. There was a low number of larva produced from the *cg-GAL4* males to *w; UAS-dBlimp-1(XA)* females cross, so only the *w; UAS-dBlimp-1(XA)* males to *cg-GAL4* females cross was used to collect samples.

Dissection of prepupae

Zero hour APF prepupae were collected in order to age to 8, 10 and 12 hours APF. Five to six prepupae were collected of each genotype for every time point. The experiment was replicated 3 times for all 3 wild-type time points (total of 9 samples), 5 times for transgenic animals at 8 and 10 hours APF, and 4 times for transgenic animals at 12 hours APF. This was due to time constraints and did not affect the study. The total number of samples was 23. The fat body was

dissected using 0.10mm x 0.06mm Dumostar #5 tweezers and collected into microfuge tubes containing 30 μ l of 1x phosphate buffered saline (PBS).

RNA isolation

After dissection, the samples were homogenized in 300 μ l of TRIzol reagent from Life Technologies, and frozen at -80°C . The samples were later thawed and transferred into 2 ml phase lock gel-heavy tubes from 5PRIME. The tubes were pre-spun at 12,000 rpm for one minute. 60 μ l of chloroform were added to the sample and centrifuged at 12,000 rpm for 10 minutes at 4°C . As a result of centrifugation, the RNA was separated by a layer of gel from the DNA, TRIzol and protein components of the sample. The separation was successful if there was a clear layer of RNA on top of a cloudy gel layer and a bottom pink TRIzol layer. An additional 60 μ l of chloroform were added to unsuccessfully separated samples and re-spun. The top clear layer of RNA was transferred to nuclease-free microfuge tubes, and 160 μ l of isopropanol were added to the sample and mixed by repeated inversion. The samples were stored overnight at -20°C .

The samples were centrifuged the next day for 20-30 minutes at 4°C at 13,400 rpm. A small pellet was visible at the bottom of the tube after spinning. The supernatant was pipetted out, and the pellet was washed with 500 μ l of 75% ethanol and spun at 4°C for 10 minutes at 13,400 rpm. At the end of the spin, the pellet was still visible. The supernatant ethanol was removed and the pellet was

allowed to air dry for 1-2 minutes. It was then resuspended in 5 μ l of nuclease-free water and incubated at 55°C for 10 minutes to facilitate diffusion. It was then vortexed and spun down, and left for five minutes at room temperature before freezing at -80°C. The samples were thawed out the next day and RNA concentration was measured using the ThermoScientific NanoDrop 2000c spectrophotometer. 1 μ l of each sample was used, and 260/280 value, 260/230 value, absorbance curve, and overall nucleotide concentration values were recorded.

Removal of contaminating DNA with DNase treatment

DNase treatment was performed with the Ambion DNA-free DNase treatment, with all reagents thawed and vortexed. To each sample, 1 μ l of 10x DNase buffer and 1 μ l of rDNase-I were added and then incubated for 25-30 minutes at 37°C. After incubation, 2 μ l of DNase inactivation reagent were added and the samples were kept at room temperature for 2 minutes, during which they were vortexed and spun down twice. The samples were then centrifuged for 90 seconds at 10,000 rpm. The resulting supernatant containing RNA was then transferred to fresh nuclease-free microcentrifuge tubes by pipet. The protocol was then repeated with 1.5 μ l of DNase buffer instead of 1 μ l, the rest of the procedure remaining the same. A new RNA concentration measurement was done on all the samples following the second DNase treatment. The majority of samples had a concentration of RNA of over 200 and a 260/280 value over 1.9.

First strand cDNA synthesis with Oligo(dT)

The cDNA synthesis procedure was completed with the First Strand SuperScript Reverse Transcriptase System kit for RT-PCR from Life Technologies. In order to run all reactions at the same time, mastermixes of the reagents were created. Two cDNA reactions were performed for each RNA sample, one with the reverse transcriptase enzyme, the other without to serve as a negative control during the PCR reactions. This resulted in 46 reactions.

The first master mix was comprised of the following reagents (Table 1) with the quantities multiplied for 46 reactions. Tubes were labeled with the RNA sample name and “RT” or “- RT” to differentiate between samples with reverse transcriptase enzyme and negative control. 1 μ l of RNA was added to each tube along with 9 μ l of the master mix. The samples were incubated at 65°C for 5 minutes, after which they were kept on ice for 1 minute.

Table 1. Master mix 1 of cDNA synthesis

Reagent	Volume for 1 reaction (μl)
10 mM dNTP Mix	1
Oligo (dT) Primer	1
DEPC-Treated water	7

A second master mix was prepared with the following reagents in the indicated order (Table 2). 9 μ l of this master mix were added to each of the RNA/master mix 1 tubes and were mixed and incubated for 2 minutes at 42°C. After incubation, 1 μ l of the reverse transcriptase enzyme SuperScript II RT was added to each “RT” labeled tube, and 1 μ l of DEPC-treated water was added to the “-RT” labeled tubes. All 46 samples were incubated for 50 minutes at 42°C to facilitate cDNA synthesis. To terminate the reaction, the samples were incubated for 15 minutes at 70°C, after which they were placed on ice. The samples were spun down after chilling, and 1 μ l of Rnase H was added to each one. They were incubated a last time for 20 minutes at 37°C. Resulting cDNA was stored at -20°C until needed for PCR.

Table 2. Master mix 2 of cDNA synthesis

Reagent	Volume for one reaction (μl)
10x RT Buffer	2
25 mM MgCl ₂	4
0.1 M DTT	2
RNase OUT	1

Primer Design

In this study, *Actin5c* and *Mmp2* amplification primers were used (Table 3). *Actin5c* is a housekeeping gene and was used as a reference point. Housekeeping genes are guaranteed present in all living cells under any experimental condition, as they are necessary for cell survival (Pfaffl, 2001). The primers used were provided by the previous students of Woodard lab and Integrated DNA Technologies (IDT) (Pohl, 2014).

Table 3. Primer sequences for *Actin5c* and *Mmp2*

Gene	Primer ID	Sequence
<i>MMP2</i>	Forward	5'-AGCAATCCGGAGTCTCCAGTCTTT-3'
	Reverse	5'-TGGAGCCGATTTTCGTGATACAGGT-3'
<i>Actin5c</i>	Forward	5'-TCTACGAGGGTTATGCCCTT-3'
	Reverse	5'-GCACAGCTTCTCCTTGATGT-3'

Reverse Transcriptase PCR (RT-PCR)

Reverse transcriptase polymerase chain reaction (RT-PCR) was used in order to determine successful cDNA synthesis of *Mmp2* and *Actin5c*. Two master mixes were prepared, one to amplify *Actin5c* cDNA, the other for *Mmp2* cDNA. The mix reagents were again multiplied to accommodate both “RT” and “-RT” tubes (Table 4). PCR tubes were labeled with the sample names, as well as target

gene and “RT” or “-RT”. 48 μ l of appropriate master mix were added to each 2 μ l of cDNA.

Table 4. RT-PCR reaction mix

Reagent	Amount per reaction	Final concentration
10x PCR Buffer-MgCl ₂	5 μ l	1X
50mM MgCl ₂	3 μ l	3 mM
10mM dNTPs	1 μ l	200 nM
10 μ M <i>Mmp2</i> or <i>Actin5c</i> forward primer	2 μ l	400 nM
10 μ M <i>Mmp2</i> or <i>Actin5c</i> reverse primer	2 μ l	400 nM
cDNA	2 μ l	
Nuclease-free water	34.6 μ l	
Taq Polymerase	0.4 μ l	2 units
Final volume	50 μ l	

The PCR reactions were placed in the thermocycler for 1 hour with the temperature settings from Table 5. After cycle completion, the amplification products were viewed using Gel electrophoresis. Remaining product was stored at -20°C.

Table 5. Thermocycler profile for *Actin5c* and *Mmp2* RT-PCR amplification

Stage	Temperature (°C)	Time	Cycle count
Denaturation	95	30 seconds	35
Annealing	58.2(<i>Mmp2</i>); 55 (<i>Actin5c</i>)	30 seconds	35
Extension	72	30 seconds	35
Final extension	72	5 minutes	1
Final hold	4	-	

Gel electrophoresis

All PCR samples were used in Gel electrophoresis in order to demonstrate the presence of the genes of interest in the cDNA RT samples. Small 1.6% agarose gels (50 mL 1X TAE, 0.8g agarose, and 5 µl ethidium bromide) and large (double quantities) gels were used. The ethidium bromide serves to view the DNA bands under fluorescence, and an additional quantity was added to the positive side of the tank to achieve greater fluorescence. The gels were run in 1X TAE for 40-60 minutes at ~130 volts. To visualize the DNA bands in the gels, a Fujifilm LAS-3000 Luminescent Image Analyzer was used. The bands were compared to a DNA ladder to match up the band sizes with the base-pair length on the ladder.

Quantitative Real Time PCR (qPCR)

In order to measure the amount of cDNA present in the initial qPCR template, a gene expression quantifying method called qPCR is used (Yuan et al., 2006). This gives quantitative data representing the actual gene expression levels. There are two methods of quantification for qPCR: absolute and relative quantification. In this study, relative quantification was used, as it accounts for different amounts of fat body that were collected in the biological samples. Relative quantification was used in order to make a comparison between the target gene *Mmp2* and control gene *Actin5c*, to quantify the expression of *Mmp2* in *βftz-f1*-reduced flies as opposed to wild-type.

For this study, qPCR was run 3 times. For the first two times, the 5PRIME RealMaster SYBR ROX 2.5x master mix. The third time, the PerfeCTa SYBR Green SuperMix, ROX was used. To quantify the amount of template amplification, qPCR measures the level of fluorescence. SYBR Green binds to the double stranded DNA and only fluoresces when attached to this type of DNA, which allows for measuring the level of ds DNA in qPCR reactions (Pfaffl, 2001). In order to quantify the initial amount of cDNA present, qPCR determines how many cycles are necessary to get the initial template to reach the threshold amount necessary before entering the exponential phase of qPCR amplification. This number of cycles is known as the Ct value, and is the value used in analyzing quantifiable qPCR data. Low Ct values signify a higher cDNA level, as it would

take a lesser time to get past the threshold (Yuan et al., 2006). Ratios representing the difference in Ct values of *Mmp2* and *Actin5c* are used to analyze the data. While qPCR is more accurate than RT-PCR, it still leaves room for error, as SYBR green will attach to any double stranded DNA present, including primer dimer (Yuan et al., 2006).

Primer optimization

Using information from previous optimizations performed in the Woodard lab, calculations were carried out in order to achieve the necessary primer concentrations for a 20 μ l reaction (as recommended by the University of Massachusetts Genomic lab qPCR machine) (Papalexi, 2013)(Table 6).

Table 6. Optimal primer concentrations (Papalexi, 2013)

Primer	Optimal concentration
<i>Actin5c</i> (forward)	500 nM
<i>Actin5c</i> (reverse)	300 nM
<i>Mmp2</i> (forward)	500 nM
<i>Mmp2</i> (reverse)	500 nM

Standard curves and efficiencies for qPCR

The Pfaffl method of qPCR analysis used in this study requires including wells to generate standard curves (Pfaffl, 2001). For this, cDNA was synthesized

from 5-6 12 hours APF whole animals. The cDNA was then serially diluted from undiluted cDNA and adding nuclease-free water in 1:2 ratio dilutions. 10 µl of nuclease free water were added to 10 µl of undiluted cDNA to achieve a 1:2 dilution, adding 10 µl of the 1:2 dilution to 10µl of nuclease-free water for a 1:4 dilution, 10 µl of 1:4 dilution to 10 µl of nuclease-free water for 1:8 dilution, and 10 µl of 1:8 dilution to 10µl of nuclease-free water to get a final 1:16 dilution. Concentrations were measured with the NanoDrop spectrophotometer. These serial dilutions were used for both *Mmp2* and *Actin5c* standard curves. For each qPCR plate, 10 total wells were used for standard curve reactions. An additional 2 wells were used without any cDNA as a negative control.

The Ct values of the standard curves were plotted on the Y axis against the X axis values of the log of each cDNA dilution concentration, and the slope was used to determine the primer amplification efficiency using equation 1.

$$Efficiency = 10^{\left(-\frac{1}{slope}\right)}$$

(equation 1)

Set up of qPCR plate

A total of 60 wells were used, including 10 for standard curves and 2 for negative control (Appendix 1). Each experimental sample type was set up in 8 wells: 3 wells containing *Actin5c* primer cDNA RT and one -RT; 3 wells containing *Mmp2* primer cDNA RT and one -RT. Each well contained 18 µl

qPCR mix with the appropriate primer (tables 7 and 8), and 2 μ l of cDNA. The thermocycler profile for qPCR is presented in table 9.

Table 7. Mix of *Actin5c* reaction for qPCR

Reagent	Amount for 1 rxn
2.5 Real SYBR Green+ ROX/ PerfeCTa SYBR Green ROX	8 μ l/ 10 μ l
<i>Actin5c</i> forward primer 500 nM	1 μ l
<i>Actin5c</i> reverse primer 300 nM	0.6 μ l
cDNA	2 μ l
Nuclease free water	8.4 μ l/6.4 μ l

The protocol for the PerfeCTa SYBR Green ROX called for 10 μ l of the mix, as opposed to 8 μ l called for by the 5PRIME. In that case, the amount of water was reduced by 2 μ l.

Table 8. Mix of *Mmp2* reaction for qPCR

Reagent	Amount for 1 rxn
2.5 Real SYBR Green+ ROX/ PerfeCTa SYBR Green ROX	8 μ l/10 μ l
<i>MMP2</i> forward primer 500 nM	1 μ l
<i>MMP2</i> reverse primer 500 nM	1 μ l
cDNA	2 μ l
Nuclease free water	6 μ l

Table 9. qPCR thermocycler profile

Stage	Temp (°C)	Time	Cycle count
<i>Taq</i> activation	95	4 minutes	1 cycle
Separation	95	15 seconds	
Annealing	58	30 seconds	40 cycles
Extension	72	30 seconds	
Dissociation			1 cycle

qPCR data analysis

The data from the qPCR reactions were analyzed using the Pfaffl method (Pfaffl, 2001). While Pfaffl discusses both absolute and relative quantification, this study makes use of the relative quantification method to correct for variations in sample collection. The Pfaffl method incorporates the amplification efficiencies of the primers into the relative expression ratio equation (equation 2), thus correcting for them. The results were expressed as a ratio of ΔC_t values between *Mmp2* amplification in wild type and *βftz-fl*-reduced flies, as compared to the ΔC_t values of *Actin5c* in the same conditions, while taking the primer amplification efficiencies into consideration.

$$Ratio = \frac{(E_{target})^{\Delta C_T(\text{control-experimental})}}{(E_{reference})^{\Delta C_T(\text{control-experimental})}}$$

(equation 2)

RESULTS

Observations during dissections

While dissecting wild-type and *βftz-f1*-reduced larval fat body, some trends were observed. In the wild-type dissections, fat body remodeling was observed clearly at 8, 10 and 12 hours APF, defined by independently floating, spherical fat body cells. At 8 hours APF, fat body remodeling in wild-type animals was observed as sheets of polygonal cells, with minimal free floating cells. At 10 hours APF, fat body remodeling in wild-type animals was observed as a mixture of both free floating cells and connected polygonal or spherical cells that were in the process of remodeling. In wild-type animals at 12h APF, fat body remodeling was observed as nearly entirely all fat body cells being free floating and spherical. Overall, in wild-type animals, fat body remodeling progressed normally from earlier to later hours APF.

During *βftz-f1*-reduced fat body dissections, less remodeling was observed overall, and especially in younger prepupae. At 8 hours APF in *βftz-f1*-reduced animals, the larval fat body was almost entirely present in sheets of cells, with minimal signs of remodeling. At 10 hours APF in *βftz-f1*-reduced animals, the larval fat body continued to show minimal signs of detachment, with most fat body cells showing no signs of remodeling. The detached cells were not spherical, but maintained a flat, polygonal shape. At 12 hours APF, the fat body in *βftz-f1*-

reduced animals showed partial signs of remodeling. As opposed to wild-type 12 hours APF, the *βftz-fl*-reduced animals showed only some fat body dissociation and detachment with spherical cells. These findings are consistent with published research (Bond et al., 2011).

Visualization of PCR products via gel electrophoresis

I used gel electrophoresis in order to visualize the RT-PCR products, testing the success of the PCR primers, cDNA synthesis and the presence of the target genes. PCR was successful at all times points in both wild-type and transgenic samples. PCR amplification was also visible at all time points, with both *Actin5c* and *Mmp2* transcripts being successfully amplified.

Actin5c samples were successfully amplified in 8, 10, and 12 hours APF wild-type and *βftz-fl*-reduced cDNA (Figures 8 and 9). The bands returned for *Actin5c* were not very bright, but they showed successful amplification. Some primer dimer is observed in all wells, and very faint bands are also visible in the no RT wells. *Mmp2* was also successfully amplified in all time points in both wild-type and *βftz-fl*-reduced samples. The bands observed for *Mmp2* in both genotypes were very bright (Figures 10 and 11). Some primer dimer is observed in all wells, and faint bands are also seen in the no RT lanes. The sample numbers are noted in the annex.

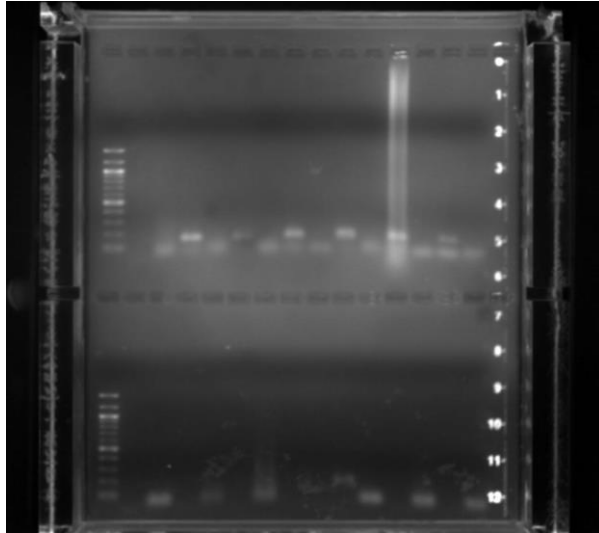


Figure 8. Gel electrophoresis of Actin5c primer samples. First row shows samples 1 through 7, second row shows samples 8 through 14.

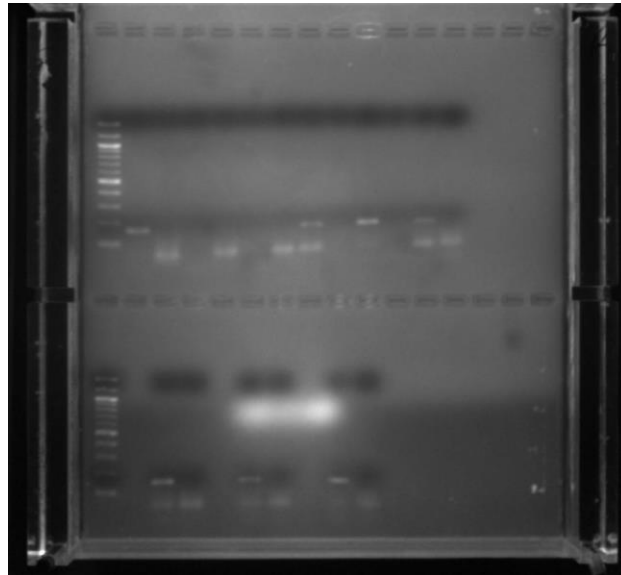


Figure 9. Gel electrophoresis of Actin5c primer samples. First row shows samples 15 through 20, second row shows samples 21 to 23.

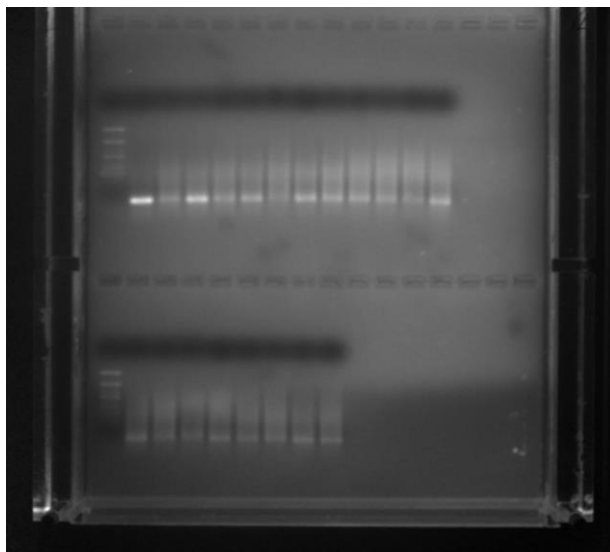


Figure 8. Gel electrophoresis of MMP2 primer samples. First row shows samples 1-4, 7-9. Second row shows samples 11-14. Samples 5,6,8 and 10 were depleted in earlier unsuccessful trials.

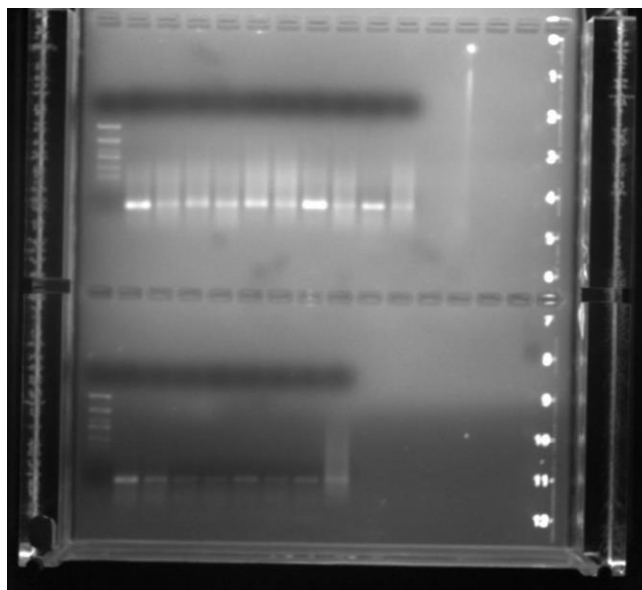


Figure 9. Gel electrophoresis of MMP2 primer samples. First row shows samples 15 through 19, second row shows samples 20 through 23.

Quantitative Real-Time PCR standard curves and primer efficiencies

The Pfaffl method was used to correct for the efficiency of the primers, which required the generation of standard curves for *Actin5c* and *Mmp2* template amplification, using serial dilutions of cDNA from wild-type whole animal aged to 12h APF. The standard curves were included on the qPCR plates, which allowed for their use as valid determinant of the efficiency of amplification. To generate standard curves, five serial dilutions were conducted (1:1, 1:2, 1:4, 1:8, 1:16). A sample slope of the standard curve for *Actin5c* was -2.92 (Figure 12).

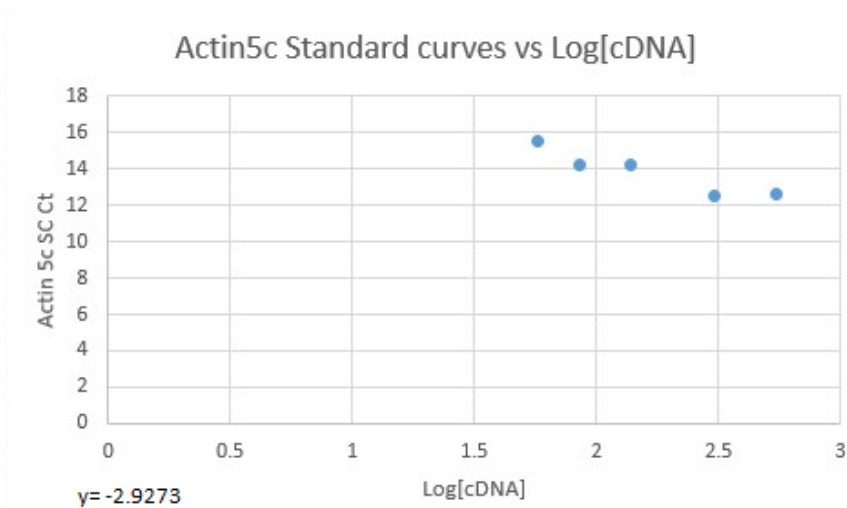


Figure 12. Standard curve of *Actin5c*. The curve was generated by plotting the Ct values of each standard curve well sample against the log of the concentration of cDNA used in each well.

This slope shows an efficiency of 2.20, which was calculated using equation 1.

A sample of a standard curve slope for *Mmp2* was -3.54 (Figure 13). The efficiency calculated using the first equation was found to be 1.91.

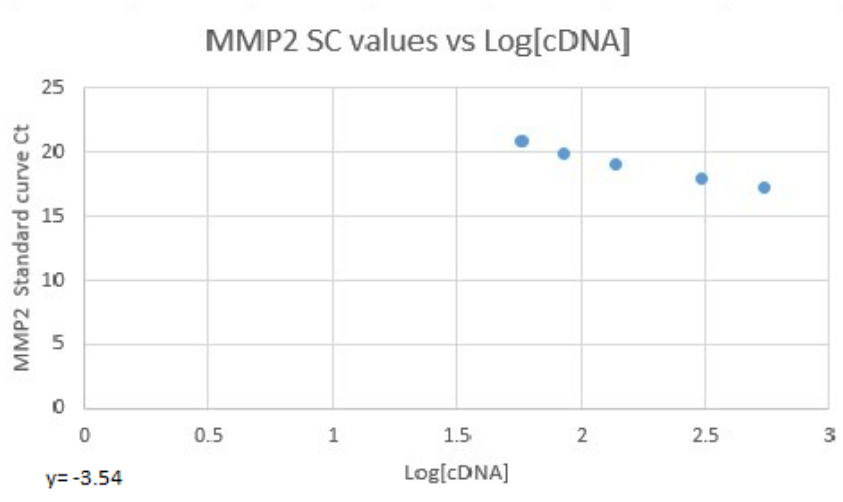


Figure 13. Standard curve of *Mmp2*. The curve was generated by plotting the Ct values of each standard curve well sample against the log of the concentration of cDNA used in each well.

An efficiency of 2 is ideal in the Pfaffl method, and deviations can indicate pipetting error or sample quality. The efficiencies found in these studies were not exactly 2, however they are acceptable.

Expression ratios of qPCR results

To determine if qPCR results are statistically significant, a one sample t-test was performed. The hypothesis was that the expression ratio of wild-type would be 1, and not 1 for transgenic animals. The mean, standard deviation, standard error mean, and p-value were calculated. Statistically significant results were those that had a p-value of less than 0.05.

The expectation was to see down-regulation of *Mmp2* expression in *βftz-fl*-reduced fat body at 8, 10 and 12 hours APF compared to wild-type. In the Pfaffl method, the expression ratio in wild-type is always 1. Expression ratios

over 1 indicate an over-expression, and under 1 indicate under-expression. At 8 hours APF, the expression ratio was 0.92 indicating a very slight under expression of *Mmp2* in *βftz-fl*-reduced fat body. The statistical analysis shows p-value = 0.185, therefore not statistically significant. Thus the expression ratio of *βftz-fl* in the larval fat body overexpressing *dBlimp-1* at 8 hours APF is equivalent to that of wild-type. At 10 hours APF, the expression ratio was 0.85 indicating a slight under expression of *Mmp2* in *βftz-fl*-reduced animals. The statistical analysis shows p-value = 0.015, which is statistically significant. At 12 hours APF, the expression ratio was 1.54 indicating slight over expression of *Mmp2* in *βftz-fl*-reduced. The statistical analysis shows p-value = 0.023, which is also statistically significant. These results are presented in a figure comparing wild-type with transgenic expression ratios (Figure 14).

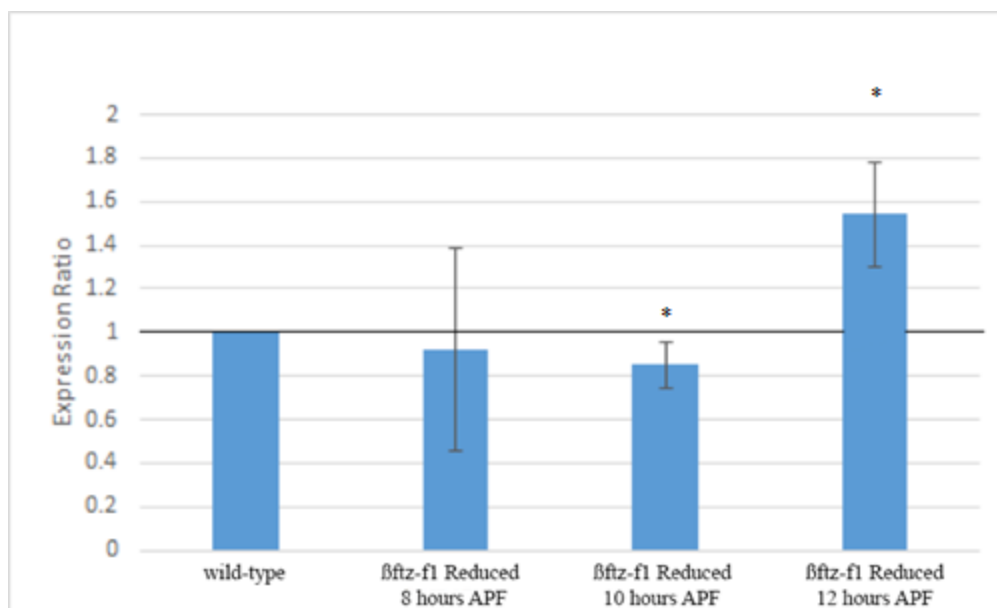


Figure 14. Expression ratios of *Mmp2* from qPCR experiments. The figure compares the expression ratios of *Mmp2* against those of *Actin5c* in $\beta ftz-f1$ -reduced compared to wild-type. Wild-type ratios are presented as 1. At 8 hours APF, the slight under expression is not statistically significant. At 10 hours APF, the expression ratios are slightly lower than 1, indicating under-expression of *Mmp2*, which is statistically significant. At 12 hours APF, the expression ratio of *Mmp2* is greater than 1, indicating an over-expression of *Mmp2* in the larval fat body, also statistically significant. Statistical significance was considered at $p < 0.05$.

DISCUSSION

Dissection observations

During dissections of both w^{1118} and $\beta ftz-f1$ - reduced fat body, several observations were made at all three time points. The trend in w^{1118} was generally showing positive correlation increasing in fat body remodeling with time. This is consistent with the known progression of wild-type remodeling. The trend in $\beta ftz-f1$ - reduced dissections also showed positive correlation, with fat body remodeling happening at a much more reduced rate but complete remodeling was not observed. Even at 12 hours APF, the $\beta ftz-f1$ - reduced dissections only showed partial remodeling, whereas in w^{1118} at 12 hours APF, fat body remodeling was nearly fully complete. This is all consistent with published research (Bond et al., 2011).

The observations made during dissection support my hypothesis: $\beta ftz-f1$ - reduced animals showed reduced larval fat body remodeling which suggests that delaying or reducing the expression of $\beta ftz-f1$ inhibits the process of remodeling, at least in part. The observations do not specifically show that the inhibition happened due to the proposed transcriptional cascade, in which $\beta FTZ-F1$ confers competence to $Mmp2$ in order for it to be able to respond to the prepupal ecdysone pulse.

Reverse-Transcriptase PCR and gel electrophoresis

RT-PCR and gel electrophoresis were overall successful. Some of the PCR reactions were amplified much stronger than others, which is visualized via gel electrophoresis as difference in band brightness. This varied strength in the gel visualization cannot be used as quantifiable data, the only conclusions to be drawn being the presence of both *Mmp2* and *Actin5c* transcripts in all samples, as well as the success of both primer design and cDNA synthesis. All gels showed both *Mmp2* and *Actin5c* amplification bands, however with varying strength. This demonstrates the presence of mRNA from both genes. I used the samples with the most clearly defined bands in qPCR.

While successful cDNA amplification was eventually obtained, it initially proved quite difficult. Amplification of *Actin5c* was successful in every trial, however *Mmp2* amplification was not observed in gel electrophoresis in the first two attempts. After the first attempt, different *Mmp2* primers were used, but these did not help in visualizing the product. After the second attempt, the annealing temperature for *Mmp2* was changed from 55°C to 58.2°C (Bond et al., 2011). This proved successful and the presented *Mmp2* gels resulted.

Quantitative Real-Time PCR results

Analysis of qPCR data showed statistically relevant down-regulation of *Mmp2* in *βftz-f1*- reduced fat body at 10 hours APF. Data also showed over

expression of *Mmp2* at 12 hours APF, and no statistical change at 8 hours APF which was unexpected. Nearly all samples returned normal dissociation curves with single peaks, suggesting no primer dimer interruption. The samples that did show multiple peaks were surprisingly empty or no RT wells.

The down ratio seen in 8 hours APF comes after two trials of results showing slight over expression and one trial that brought the average down under 1. Since the method of quantification used is relative, it cannot be concluded with certainty that this level of expression is equivalent to that of wild type at its peak. This variation might be due to pipetting errors in the final qPCR plate, and is not statistically relevant. The other two time points were consistent in results.

At 12 hours APF, the slight over expression might be due to the time of retrieval of data. I believe that *βftz-f1* is delayed past this window and levels of *Mmp2* show as over expressed during this time as compared to wild-type (Figure 15). This may be because in *βftz-f1*-reduced larval fat bodies, the peak of *Mmp2* expression is delayed until 12 hours APF, at which point the expression of *Mmp2* in wild-type larval fat body has already peaked and is declining.

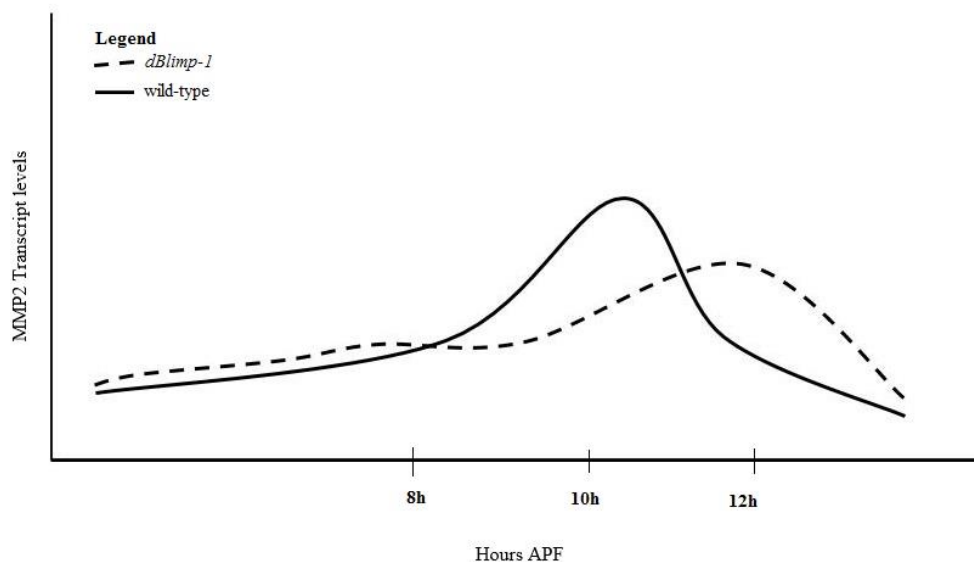


Figure 15. Proposed expression levels of *Mmp2*. The graph shows the level of *Mmp2* transcript at 8, 10 and 12 hours APF. At 12 hours APF we see slight over-expression in transgenic flies as opposed to wild-type. This may be because in $\beta ftz-f1$ -reduced larval fat bodies, the peak of *Mmp2* expression is delayed until 12 hours APF, at which point the expression of *Mmp2* in wild-type larval fat body is already declining.

While my hypothesis is not fully supported by the results, there was a difference between *Mmp2* expression levels in wild-type and $\beta ftz-f1$ -reduced flies at all time points, even though these differences did not always show a reduction of expression. These results do show a regulatory connection between $\beta ftz-f1$ and *Mmp2*. The levels of *Mmp2* were altered in transgenic animals in which *dBlimp-1* was over expressed in the larval fat body, with no experimental alteration done on *Mmp2*. Previous Woodard lab research showed a statistically significant reduction of $\beta ftz-f1$ expression in the transgenic flies used in this experiment (Perez, 2014). Since *dBlimp-1* is known to be a $\beta ftz-f1$ repressor, it can be assumed that these

experimental alterations led to changes in *βftz-f1* expression levels which in turn contributed to the observed variation in fat body remodeling and *Mmp2* variations in these transgenic animals.

With this knowledge, it can be said that this study demonstrates the correlation between altering the expression levels of *βftz-f1* and the alteration of *Mmp2* expression levels in *Drosophila melanogaster* larval fat body. Since both wild-type and *βftz-f1*- reduced animals underwent the same experimental procedures, it was the over expression of *dBlimp-1* and consequently the reduction in *βftz-f1* expression that affected the expression of *Mmp2*.

Delayed expression of *βftz-f1* disrupts normal development

Since expression level and timing of *βftz-f1* is so crucial, the delayed expression should result in abnormal metamorphic processes. Metamorphosis is the time in which a large number of nuclear receptors are expressed, and their expression is regulated by ecdysone (Thummel, 1995). The successfulness of this ecdysone cascade is reliant upon the expression of the correct gene, at the right time and in the right amount. If these parameters are off, the subsequent steps in the cascade are disrupted. Thus, given the fact that *βftz-f1* is believed to be involved in the expression of *Mmp2* and in fat body remodeling, precise timing is crucial. Without it, *Mmp2* expression is unlikely to occur.

Relationship between human health and larval fat body remodeling

In order to get important insight into the control of development of *Drosophila*, we study the process of fat body remodeling. However, this can be used to get valuable insight into human health as well. During the remodeling process, the fat body goes through a change that allows the fat body cells to move freely through the body cavity. While humans don't have a homologous process, human tissue does undergo remodeling with the help of MMPs. The 23 MMPs of humans play a role in cancer metastasis, wound healing, and central nervous system processes (Malemud, 2006).

Matrix Metalloproteinases and human health

Wound healing is a complex process that we can divide into three stages: inflammatory response, proliferation, and remodeling (Li et al., 2007). In the proliferation stage, MMPs degrade the connections between keratinocytes, which migrate, proliferate, and differentiate in order to help restore the tissue (Li et al., 2007). During the remodeling stage, new tissue restores functional competence and structural integrity.

In the case of cancer metastasis, there are two MMPs that are primarily responsible for degrading the protein components of the ECM holding the tumor cells together, thus allowing for these cells to freely migrate to the blood stream and to the rest of the body (Malemud, 2006). The MMPs are also responsible for

stimulating angiogenesis, which allows for the continued growth of the tumor (Malemud, 2006). There is some evidence that high levels of MMP expression are associated with advanced cancer, thus MMPs may contribute to the progression of cancer (Fingleton, 2003).

The role of MMPs in cancer is very complex and depends on the specific MMPs present and the stage the cancer is in, as different MMPs play different roles at different stages of cancer. For example, MMP-8 provides a protective effect during the metastatic process, diminishing the metastatic potential when it is overexpressed. MMP-8 has been associated with improved survival in the case of some cancers (Gialeli et al., 2011). Another example is MMP-9 which can act as a tumor promoter during carcinogenesis, but also as an anticancer enzyme during later stages (Gialeli et al., 2011). It is clear that understanding the function of MMPs is very important in understanding the ways in which cancers spread and advance, and in trying to devise ways of treatment.

In the central nervous system (CNS), MMPs play a very important role, as they are responsible for the regulation of the destruction and remodeling of the ECM proteins, as well as mediation of the disruption of the blood brain barrier (Malemud, 2006). According to Malemud (2006), MMPs appear to regulate nervous tissue injury from MS, Alzheimer's disease, and meningitis. They are also known for their negative effects in brain injury and disease, as they contribute to the loss of neurons and synaptic damage (Huntley, 2012).

Upregulation of MMPs has been associated with diseases in the CNS. For example, upregulation of MMP-9 promotes the development and progression of diseases, but MMP-12 can actually help to resolve the issue (Yong, 2005). While the bad effects of MMPs are numerous and documented, they can also have a positive impact regarding growth and regeneration in processes like neurogenesis and myelinogenesis (Yong, 2005).

Conclusion

Results from qPCR analysis support my hypothesis at 10 hours APF. This study continues the work of a previous Woodard lab student who found under expression only at 10 hours APF (Katz, 2015), but the findings are still highly preliminary. Visualization of the qPCR dissociation curves shows mostly single peaked samples, which leads to the belief that the primer optimization was correct and that the results are relatively reliable.

These results do not objectively support the hypothesis that *Mmp2* is a downstream regulatory target of *βftz-f1* in the larval fat body remodeling process. The results however suggest that expression of *Mmp2* is delayed in *βftz-f1*-reduced animals, supporting the hypothesis that proper *Mmp2* transcription is dependent on *βftz-f1*.

Future directions

Future studies should look into using Western blotting in order to look at 12 hours APF expression ratios more closely. Due to our belief that over expression is seen due to the delayed expression of *βftz-f1* as compared to wild-type, a closer look might be able to more accurately show what the expression levels are.

APPENDIX

Appendix 1. qPCR plate setup

	1	2	3	4	5	6	7	8	9	10	11	12
A	Standard 1:1 Actin 5c	Standard 1:2 Actin 5c	Standard 1:4 Actin 5c	Standard 1:8 Actin 5c	Standard 1:16 Actin 5c	Blank	Blank	Blank	Blank	Blank	Blank	Blank
B	Standard 1:1 Mmp2	Standard 1:2 Mmp2	Standard 1:4 Mmp2	Standard 1:8 Mmp2	Standard 1:16 Mmp2	Blank	Blank	Blank	Blank	Blank	Blank	Blank
C	w^{1118} 8h Actin 5c RT	w^{1118} 8h Actin 5c RT	w^{1118} 8h Actin 5c RT	w^{1118} 8h Actin 5c no RT	Blank	Blank	Blank	Blank	β ftz-f1- reduced 8h Actin 5c RT	β ftz-f1- reduced 8h Actin 5c RT	β ftz-f1- reduced 8h Actin 5c RT	β ftz-f1- reduced 8h Actin 5c no RT
D	w^{1118} 8h Mmp2 RT	w^{1118} 8h Mmp2 RT	w^{1118} 8h Mmp2 RT	w^{1118} 8h Mmp2 no RT	Blank	Blank	Blank	Blank	β ftz-f1- reduced 8h Mmp2 RT	β ftz-f1- reduced 8h Mmp2 RT	β ftz-f1- reduced 8h Mmp2 RT	β ftz-f1- reduced 8h Mmp2 no RT
E	w^{1118} 10h Actin 5c RT	w^{1118} 10h Actin 5c RT	w^{1118} 10h Actin 5c RT	w^{1118} 10h Actin 5c no RT	Blank	Blank	Blank	Blank	β ftz-f1- reduced 10h Actin 5c RT	β ftz-f1- reduced 10h Actin 5c RT	β ftz-f1- reduced 10h Actin 5c RT	β ftz-f1- reduced 10h Actin 5c no RT
F	w^{1118} 10h Mmp2 RT	w^{1118} 10h Mmp2 RT	w^{1118} 10h Mmp2 RT	w^{1118} 10h Mmp2 no RT	Blank	Blank	Blank	Blank	β ftz-f1- reduced 10h Mmp2 RT	β ftz-f1- reduced 10h Mmp2 RT	β ftz-f1- reduced 10h Mmp2 RT	β ftz-f1- reduced 10h Mmp2 no RT
G	w^{1118} 12h Actin 5c RT	w^{1118} 12h Actin 5c RT	w^{1118} 12h Actin 5c RT	w^{1118} 12h Actin 5c no RT	Blank	Blank	Blank	Blank	β ftz-f1- reduced 12h Actin 5c RT	β ftz-f1- reduced 12h Actin 5c RT	β ftz-f1- reduced 12h Actin 5c RT	β ftz-f1- reduced 12h Actin 5c no RT
H	w^{1118} 12h Mmp2 RT	w^{1118} 12h Mmp2 RT	w^{1118} 12h Mmp2 RT	w^{1118} 12h Mmp2 no RT	Blank	Blank	Blank	Blank	β ftz-f1- reduced 12h Mmp2 RT	β ftz-f1- reduced 12h Mmp2 RT	β ftz-f1- reduced 12h Mmp2 RT	β ftz-f1- reduced 12h Mmp2 no RT

Appendix 2. Table of numbered samples corresponding to the genotype and hour of collection

Sample #	Genotype	hours APF
1	w ¹¹¹⁸	8
2	w ¹¹¹⁸	8
3	w ¹¹¹⁸	8
4	w ¹¹¹⁸	10
5	w ¹¹¹⁸	10
6	w ¹¹¹⁸	10
7	w ¹¹¹⁸	12
8	w ¹¹¹⁸	12
9	w ¹¹¹⁸	12
10	cg-GAL4;UAS-dBlimp-1	8
11	cg-GAL4;UAS-dBlimp-1	8
12	cg-GAL4;UAS-dBlimp-1	8
13	cg-GAL4;UAS-dBlimp-1	8
14	cg-GAL4;UAS-dBlimp-1	8
15	cg-GAL4;UAS-dBlimp-1	10
16	cg-GAL4;UAS-dBlimp-1	10
17	cg-GAL4;UAS-dBlimp-1	10
18	cg-GAL4;UAS-dBlimp-1	10
19	cg-GAL4;UAS-dBlimp-1	12
20	cg-GAL4;UAS-dBlimp-1	12
21	cg-GAL4;UAS-dBlimp-1	12
22	cg-GAL4;UAS-dBlimp-1	12
23	cg-GAL4;UAS-dBlimp-1	12

LITERATURE CITED

- Agawa, Y., Sarhan, M., Kageyama, Y., Akagi, K., Takai, M., Hashiyama, K., Wada, T., Handa, H., Iwamatsu, A., Hirose, S., and Ueda H. (2007). *Drosophila* Blimp-1 is a transient transcriptional repressor that controls timing of the ecdysone-induced developmental pathway. *Molecular and Cellular Biology*, 27 (24), 8739-8747.
- Aguila, J.R., Hoshizaki, D.K., Gibbs, A.G., 2013. Contribution of Larval Nutrition to Adult Reproduction in *Drosophila melanogaster*. *The Journal of Experimental Biology* 216, 399-406.
- Aguila, J. R., Suszko, J., Gibbs, A. G., and Hoshizaki, D. K. (2007). The role of larval fat cells in adult *Drosophila melanogaster*. *The Journal of Experimental Biology*, 210, 956-963.
- Akagi, K. and Ueda, H. (2011). Regulatory mechanisms of ecdysone-inducible Blimp-1 encoding a transcriptional repressor that is important for the prepupal development in *Drosophila*. *Development, Growth & Differentiation*, 53, 697– 703.
- Bainbridge, S. P., and Bownes, M. (1981). Staging the metamorphosis of *Drosophila melanogaster*. *Journal of embryology and experimental morphology*, 66.1, 57-80.
- Bond, N. Nelliott, A., Bernardo, M.D., **Gorski, K., **Ayerh, M., Hoshizaki, D.K. and Woodard, C.T. (2011). β FTZ-F1 and Matrix metalloproteinase 2 are required for fat-body remodeling in *Drosophila*. *Developmental Biology*, 360, 286-296.
- Broadus, J., McCabe, J.R., Endrizzi, B., Thummel, C.S., and Woodard, C.T., (1999). The *Drosophila* β FTZ-F1 orphan nuclear receptor provides competence for stage-specific responses to the steroid hormone ecdysone. *Mol. Cell*, 3, 143-149.
- Fingleton, B., 2003. Matrix Metalloproteinase Inhibitors for Cancer Therapy: The Current Situation and Future Prospects. *Expert opinion on therapeutic targets* 7, 385-397.

- Fortier, T.M., Vasa, P.P., and Woodard, C.T. (2003). Orphan nuclear receptor β FTZ- F1 is required for muscle-driven morphogenetic events at the prepupal– pupal transition in *Drosophila melanogaster*. *Dev Biol.* 257, 153-165.
- Géminard, C., Rulifson, E. J., and Léopold, P. (2009). Remote control of insulin secretion by fat cells in *Drosophila*. *Cell metabolism* 10.3, 199-207.
- Gialeli, C., Theocharis, A.D., and Karamanos, N.K. (2011). Roles of Matrix metalloproteinases in cancer progression and their pharmacological targeting. *FEBS Journal*, 278, 16-27.
- Guichet, A., Copeland, J.W., Erdélyi, M., Hlousek, D., Závorszky, P., Ho, J., Brown, S., Percival-Smith, A., Krause, H.M., Ephrussi, A., 1997. The Nuclear Receptor Homologue Ftz-F1 and the Homeodomain Protein Ftz are Mutually Dependent Cofactors.
- Hoshizaki, D., 2005. Fat-Cell Development. *Comprehensive molecular insect science* 2, 315-345.
- Huntley, G.W., 2012. Synaptic Circuit Remodeling by Matrix Metalloproteinases in Health and Disease. *Nature Reviews Neuroscience* 13, 743-757.
- Hyun-Jeong, R., and Parks W. C. (2007). Control of Matrix metalloproteinase catalytic activity. *Matrix Biology* 26.8, 587-96.
- Jia, Q., Liu, Y., Liu, H., & Li, S. (2014). Mmp1 and Mmp2 cooperatively induce *Drosophila* fat body cell dissociation with distinct roles. *Scientific Reports*, 4, 7535.
- Kessenbrock, K., Plaks, V., and Werb, Z. (2010) Matrix metalloproteinases: regulators of the tumor microenvironment. *Cell*, 141.1, 52-67.
- Kozlova, T, and Thummel, C. S. (2003). Essential roles for ecdysone signaling during *Drosophila* mid-embryonic development. *Science*, 301.5641 1911-914.
- Lavorgna, G., Ueda, H., Clos, J., Wu, C., 1991. FTZ-F1, a Steroid Hormone Receptor-Like Protein Implicated in the Activation of Fushi Tarazu. *Science* 252, 848-851.
- Lee, C., Simon, C.R., Woodard, C.T., Baehrecke, E.H., 2002b. Genetic Mechanism for the Stage-and Tissue-Specific Regulation of Steroid Triggered Programmed Cell Death in *Drosophila*. *Dev Biol* 252, 138-148.
- Li, J., Chen, J., Kirsner, R., 2007. Pathophysiology of Acute Wound Healing. *Clin Dermatol* 25, 9-18.
- Liu, Y., Liu, H., Liu, S., Wang, S., Jiang, R., Li, S., 2009. Hormonal and Nutritional Regulation of Insect Fat Body Development and Function. *Arch Insect Biochem Physiol* 71, 16-30.
- Lu, P., Takai, K., Weaver, V. M., and Werb, Z. (2011). Extracellular matrix

- degradation and remodeling in development and disease. *Cold Spring Harbor Perspectives in Biology* 3.12.
- Malemud, C.J., 2006. Matrix Metalloproteinases (MMPs) in Health and Disease: An Overview. *Front Biosci* 11, 1696-1701.
- Nelliot, A., Bond, N., and Hoshizaki, D. K. (2006). Fat-body remodeling in *Drosophila melanogaster*. *Genesis*, 44(6), 396-400.
- Ou, Q., King-Jones, K., 2013. What Goes Up must Come Down: Transcription Factors have their Say in Making Ecdysone Pulses. *Curr Top Dev Biol* 103, 35-71.
- Page-McCaw, A. (2008). Remodeling the model organism: Matrix metalloproteinase functions in invertebrates. *Seminars in Cell & Developmental Biology*, 19, 14-23.
- Page-McCaw, A., Ewald, A. J., and Werb, Z. (2007). Matrix metalloproteinases and the regulation of tissue remodeling. *National Review of Molecular Cell Biology*, 8, 221- 233.
- Perez, L. (2014). The effects of β ftz-f1 in *Drosophila melanogaster* larval fat body remodeling. Unpublished Bachelors of Arts, Mount Holyoke College.
- Pohl, N. (2014). The Role of MMP2 in *Drosophila melanogaster* fat body remodeling. Unpublished Bachelors of Arts, Mount Holyoke College.
- Qiangqiang, J., Yang, L., Hanhan, L., and Sheng, L. (2014). Mmp1 and Mmp2 cooperatively induce *Drosophila* fat body cell dissociation with distinct roles. *Scientific Reports*, 4 (7535).
- Shresthak, Y. (2005). Molecular Mechanisms Underlying the Regulation of the *Drosophila* E93 Gene by Ecdysone and β ftzf1. Unpublished Bachelors of Arts, Mount Holyoke College.
- Søndergaard, L., 1993. Homology between the Mammalian Liver and the *Drosophila* Fat Body. *Trends in Genetics* 9, 193.
- Spindler, K., Hönl, C., Tremmel, C., Braun, S., Ruff, H., Spindler-Barth, M., 2009. Ecdysteroid Hormone Action. *Cellular and molecular life sciences* 66, 3837-3850.
- Stevens, L. J., and Page-McCaw, A. (2012). A secreted MMP is required for reepithelialization during wound healing. *Molecular Biology of the Cell* 23.6, 1068-079
- Thummel, C.S., 1995. From Embryogenesis to Metamorphosis: The Regulation and Function of *Drosophila* Nuclear Receptor Superfamily Members. *Cell* 83, 871-877
- Weigmann, K., Klapper, R., Strasser, T., Rickert, C., Technau, G. M., Jackle, H., Janning, W., and Klämbt, C. (2003). FlyMove: A new way to look at development of *Drosophila*. *Trends Genetics*, 19 (6), 310-311.
- Woessner, J. F. Jr. (1991) Matrix metalloproteinases and their inhibitors in connective tissue remodeling." *The FASEB Journal* 5.8, 2145-2154.

- Woodard, C. T., Baehrecke, E. H., and Thummel, C. S. (1994). A molecular mechanism for the stage specificity of the *Drosophila* prepupal genetic response to ecdysone. *Cell*, 79, 607-615.
- Yamada, M., Murata, T., Hirose, S., Lavorgna, G., Suzuki, E., and Ueda, H., (2000). Temporally restricted expression of transcription factor betaFTZF1: significance for embryogenesis, molting and metamorphosis in *Drosophila melanogaster*. *Development* 127, 5083-5092.
- Yong, V.W., 2005. Metalloproteinases: Mediators of Pathology and Regeneration in the CNS. *Nature Reviews Neuroscience* 6, 931-944